

# Determination of the Born–Oppenheimer potential function of $\text{CCl}^+$ by velocity modulation diode laser spectroscopy

Martin Gruebele, Mark Polak, Geoffrey A. Blake,<sup>a)</sup> and Richard J. Saykally<sup>b)</sup>

*Department of Chemistry, University of California, Berkeley, California 94720*

(Received 23 June 1986; accepted 12 August 1986)

Over 70 transitions among the lowest six vibrational states of  $\text{C}^{35}\text{Cl}^+$  and  $\text{C}^{37}\text{Cl}^+$  have been measured between 1070–1210  $\text{cm}^{-1}$ . The spectrum has been fitted to a sixth order Dunham expansion to yield an accurate mapping of the Born–Oppenheimer potential function of  $\text{CCl}^+$ . The spectroscopic constants obtained are  $\omega_e = 1177.7196(8) \text{ cm}^{-1}$ ,  $\omega_e x_e = 6.6475(3) \text{ cm}^{-1}$ , and  $B_e = 0.797\,940(3) \text{ cm}^{-1}$ . The rotational constants for both  $\text{CCl}^+$  isotopes reported here show the results of the previous electronic emission studies to be incorrect. A fit of the data to a Morse function yields a dissociation energy  $D$  of 52 828(50)  $\text{cm}^{-1}$ . The rotational temperature has been determined as 540 K  $\pm$  30%. The increase in the effective vibrational temperature with vibrational excitation indicates that  $\text{CCl}^+$  is formed with high internal energy.

## INTRODUCTION

Due to the ubiquitous employment of halocarbon plasmas in the processing of semiconductor materials, there is much interest in ascertaining the identity, structure, state temperatures, and spatial distributions of reactive species generated in the plasma.<sup>1</sup> This research group has concentrated on the study of charged species which are of possible importance in reactive plasma applications. To date, studies of  $\text{HF}^+$ ,  $\text{HCl}^+$ , and  $\text{HBr}^{+2-4}$  have been carried out by far infrared laser magnetic resonance spectroscopy, and  $\text{H}_2\text{F}^{+5}$  and  $\text{CF}^{+6}$  have been studied by velocity modulation infrared laser spectroscopy. In addition, Kawaguchi and Hirota have published results for  $\text{CF}^{+7}$  and  $\text{FHF}^{-8}$ , but this exhausts the list of halogen-containing ions that have been studied in detail by high resolution spectroscopic methods.

In our diode laser investigation of  $\text{CF}^+$  in a  $\text{C}_2\text{F}_6$  plasma, a very high vibrational temperature was observed (5000 K), permitting the measurement of hot bands up to  $v = 6 \rightarrow 7$ . From these extensive vibration–rotation spectra an accurate equilibrium structure and experimental potential in the form of a power series were determined for  $\text{CF}^+$ . Experimental information of this kind is rare for charged molecules, and there has been substantial interest on the part of quantum chemists in comparing calculated potential functions of simple ions with experimental results.

In this paper we present the results of a study of the two isotopic species of the  $\text{CCl}^+$  ion generated in a  $\text{He}/\text{CCl}_4/\text{CHCl}_3$  plasma by velocity modulation diode laser spectroscopy. As in the case of  $\text{CF}^+$ , a high degree of vibrational excitation is observed, permitting vibrational states up to  $v = 6$  to be measured. The equilibrium structure and Born–Oppenheimer potential function of the ion were determined by directly fitting the data to a power series potential.

The  $\text{CCl}^+$  ion has not previously been observed by high resolution methods. It was first discovered in 1954 by

Barrow and co-workers<sup>9</sup> in the emission of a  $\text{CCl}_4$  discharge and later studied by Kuzyakov and Tatevsky,<sup>10</sup> but no rotational analysis of the spectra was possible. Higher resolution emission spectra were reported by Verma in 1961<sup>11</sup> and Bredohl, Dubois, and Melen in 1983.<sup>12</sup> However, each of these studies assigned different emission features to the same  $\text{CCl}^+ A \ ^1\Pi-X \ ^1\Sigma$  band system and produced very different molecular constants for the ground state, without any distinction between the chlorine isotopes. The analysis of the vibration–rotation bands studied here, accurate to 0.003  $\text{cm}^{-1}$ , yields  $B$  values for the individual isotopes which are substantially different from those reported by both emission studies.

## EXPERIMENTAL

A diagram of the experiment is shown in Fig. 1. Modes from the Laser Analytics tunable diode laser source were collimated by an aluminum parabola and selected with a 0.3 m monochromator. Two diodes were employed to cover the frequency range from 1060 to 1210  $\text{cm}^{-1}$ . After final collimation to about 0.6 cm, the radiation was passed through a discharge cell of 1 m length and 1 cm internal diameter. Special electrodes were required to allow noise-free operation of the unstable halocarbon discharge. Each electrode consists of a Teflon disk with fittings for a replaceable water-cooled 3/8 in. copper coil. The metal coil was also partially coated with Teflon. The 25 kHz ac discharge was typically operated at 800 mA and 300 W by a Plasmaloc 2 power generator. The current waveform was maintained at approximately 30% duty cycle. Lines could be seen in either  $\text{CCl}_4$  or  $\text{CHCl}_3$  discharges, but the most intense hotbands were recorded using a 15 mTorr 50:50 mixture of  $\text{CCl}_4/\text{CHCl}_3$  in 2–2.5 Torr of He carrier gas. In argon, the signal to noise ratio was substantially reduced. The temperature of the cell was maintained below 15 °C by a closed cycle refrigerator.

After a single pass through the cell, the laser radiation

<sup>a)</sup> Berkeley Miller Postdoctoral Associate 1985–87.

<sup>b)</sup> Berkeley Miller Research Professor 1985–86.

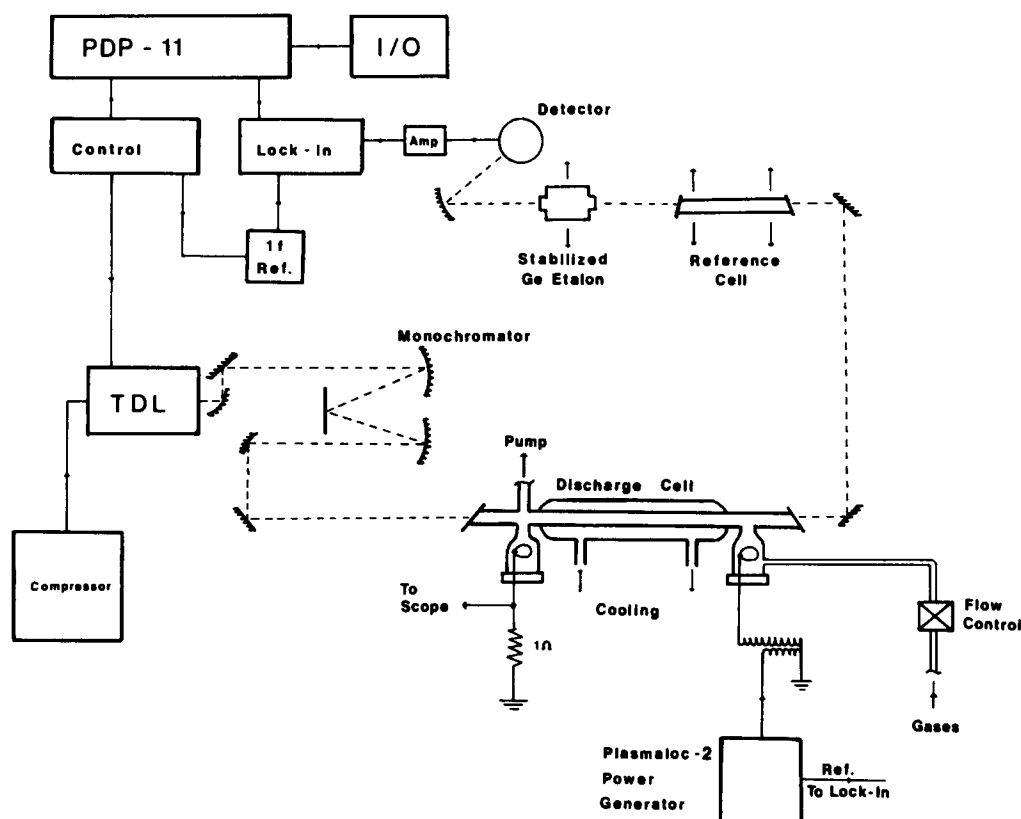


FIG. 1. Schematic diagram of the diode laser velocity modulation spectrometer.

was detected by a HgCdTe detector. The preamplifier signal was then sent to a lock-in amplifier which detected the Doppler modulated ion signals at the discharge frequency. Frequency calibration was performed with  $\text{N}_2\text{O}^{13}$  and  $\text{NH}_3^{14}$  lines using a 1 m reference cell which could be inserted into the beam path. Relative calibration was provided by a 2 in. solid Ge étalon of  $0.0163\text{ cm}^{-1}$  free spectral range temperature stabilized by an oil bath. The reference lines and étalon fringes were recorded by frequency modulation of the source at 10 kHz. All transitions were measured with a 125 ms time constant and an integration time of 1 s over the lines. The measurement precision is estimated to be  $0.003\text{ cm}^{-1}$  and is largely limited by small drifts in the laser current and temperature between data and reference scans and the uncertainty in the reference line positions.

The spectrometer is controlled by a PDP-11 microcomputer. The laser electronics have been interfaced to the computer, which automatically reads the laser current and temperature. An operating system-like program effects the collection of data, scaling of the étalon fringes to the reference lines, automatic calibration of lines and other required tasks.

## RESULTS

Low resolution emission results<sup>10</sup> were used to estimate the search region. Line densities of 3–4 per  $\text{cm}^{-1}$  were found near the predicted band center. The spectrum was then sorted by intensity and checked for line spacings of multiples of  $1.6\text{ cm}^{-1}$  by Fourier transformation. This procedure yielded three bands, the most intense of which was assigned as the fundamental of  $\text{C}^{35}\text{Cl}^+$ . A preliminary fit of 17 fundamental

lines was used to calculate  $D_e$ . This was compared to the theoretical prediction  $D_e = 4B_e^3/w_e^2$  to locate the band center within 1 quantum of the rotation. The  $\text{C}^{37}\text{Cl}^+$  fundamental was then assigned by comparing the scaled  $B$  value of the fundamental with the spacings of the other progressions, leaving the third band as  $v = 1 \rightarrow 2$  transition of the  $\text{C}^{35}\text{Cl}^+$  species. The resulting value of  $w_e x_e$  made the assignment of the remaining spectra straightforward.

A total of 70 lines has been fit to transitions involving  $v = 0-6$  in  $\text{C}^{35}\text{Cl}^+$  and  $v = 0-3$  in  $\text{C}^{37}\text{Cl}^+$ . The relative intensities of lines in the same laser modes were also determined by scaling to the intensity of the étalon fringes to eliminate the interference from incoherent background radiation. The width of the lines (HWHM) was found to be  $0.0026 \pm 0.0002\text{ cm}^{-1}$ . The first derivative line shape of the ion signals resulting from velocity modulation allowed easy distinction of the ions from interfering neutrals (Fig. 2).<sup>15</sup>

The data were fit to the Dunham expansion of the rotation-vibration energy  $E$  for diatomic molecules, including terms up to  $(r - r_e)^8$  in the potential energy ( $U$ ) power series expansion<sup>16</sup>

$$E = \sum_{p,q} Y_{pq}(w_e, B_e, a_1, \dots, a_6) \left( v + \frac{1}{2} \right)^p J^q (J+1)^q, \quad (1)$$

$$U = a_0 x^2 (1 + a_1 x + a_2 x^2 + a_3 x^3 \dots),$$

$$x = \frac{r - r_e}{r_e} \quad (2)$$

yielding values for  $B_e, w_e$ , and the potential constants  $a_1-a_6$ . Both isotopic species were fit simultaneously, by keeping the

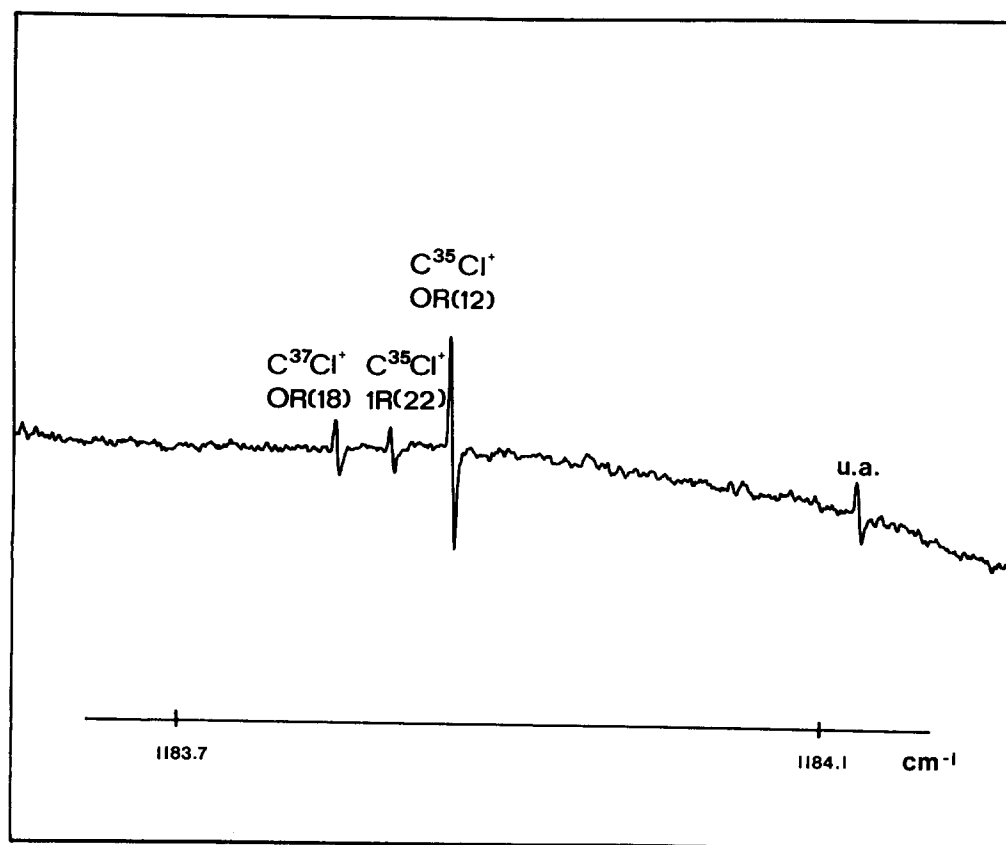


FIG. 2. Spectra from the  $\text{CCl}^+$   $R$  branch, showing lines from a hot-band and the  $\text{C}^{37}\text{Cl}^+$  isotopic species. The number before the rotational assignment represents the lower vibrational state.

potential constants the same and scaling  $B_e$  and  $w_e$  for reduced mass. The standard deviation of the fit was  $0.0021 \text{ cm}^{-1}$ . The observed lines, with assignments and residual errors are presented in Table I. The assignment given exhibits the lowest residual error and produces molecular constants of reasonable magnitudes and signs, which is not the case for slightly different rotational assignments. The resulting molecular constants are given in Table II, together with their correlation matrix. Table III presents the Dunham coefficients  $Y_{pq}$  for  $\text{C}^{35}\text{Cl}^+$ , which closely correspond to the normally quoted molecular constants ( $w_e \sim Y_{10}$ ,  $B_e \sim Y_{01}$ , etc.). They were calculated by inserting the potential constants and the isotopically scaled  $w_e$  and  $B_e$  into the standard expression for the Dunham coefficients given in Ref. 16. These constants are expected to be of similar accuracy as those of  $\text{CF}^+$ , which were used to predict the microwave results of Plummer *et al.*<sup>17</sup> to within 3 MHz.

## DISCUSSION

The rotational constants determined in this study and those from the earlier emission studies (Table IV) lie well outside their combined uncertainties. Verma and Bredohl assign the  $A \ ^1\Pi-X \ ^1\Sigma$  system to two completely different emission features, separated by  $5000 \text{ cm}^{-1}$ . In view of our data, both assignments are most likely incorrect. We hope that our rotation-vibration constants will help to clear up the confusion generated by the inconsistent optical data. The agreement of our harmonic frequency and anharmonicity

with Ref. 10 is good, considering the low precision of the previous measurements.

In order to obtain an estimate of the dissociation energy of  $\text{CCl}^+$ , and to see how a very simple analytical representation of the vibrational well fits the data, the transitions were also fit to a Morse potential with qualitatively correct behavior in the dissociation region

$$U = D(1 - e^{-ax})^2 \quad (3)$$

with the dissociation energy  $D$  given by

$$D = \frac{\omega_e^2}{4a^2 B_e}. \quad (4)$$

Taylor series expansion of the Morse potential (3) and equation of the coefficients with those of the power series expansion (2) of the potential yields the following relationships between the potential constants  $a_1$ - $a_6$  and the Morse constant  $a$ :

$$\begin{aligned} a_0 &= Da^2, \\ a_1 &= -a, \\ a_2 &= 7/12a^2, \\ a_3 &= -1/4a^3, \\ a_4 &= 31/360a^4, \\ a_5 &= -126/7!a^5, \\ a_6 &= 250/8!a^6. \end{aligned} \quad (5)$$

TABLE I. Observed transitions and assignments. Isotope 1 is C<sup>35</sup>Cl<sup>+</sup>. Frequencies are in cm<sup>-1</sup>, residual errors in 10<sup>-3</sup> cm<sup>-1</sup>.

<i>I</i>	Observed	<i>o</i> - <i>c</i>	<i>v</i> <sub>1</sub>	<i>v</i> <sub>u</sub>	<i>J</i> <sub>1</sub>	<i>J</i> <sub>u</sub>
1	1212.769	-3.7	0	1	35	36
1	1208.280	-3.6	0	1	31	32
1	1204.769	0.0	0	1	28	29
1	1201.130	1.3	0	1	25	26
1	1196.077	-4.0	0	1	21	22
1	1193.478	3.3	0	1	19	20
1	1192.155	3.9	0	1	18	19
2	1188.966	3.3	0	1	22	23
1	1188.810	1.4	1	2	26	27
1	1188.100	1.5	0	1	15	16
1	1185.330	0.8	0	1	13	14
2	1185.125	3.9	0	1	19	20
1	1183.925	0.7	0	1	12	13
1	1183.867	1.5	1	2	22	23
2	1183.815	1.1	0	1	18	19
1	1180.012	-1.8	1	2	19	20
1	1179.989	-0.3	2	3	30	31
2	1179.811	-1.1	0	1	15	16
1	1179.626	-3.4	0	1	9	10
1	1176.042	2.6	1	2	16	17
2	1175.693	1.7	0	1	12	13
1	1175.212	-2.8	0	1	6	7
1	1172.201	-4.7	0	1	4	5
2	1167.923	1.0	1	2	16	17
1	1167.895	1.0	2	3	20	21
1	1167.622	-1.0	3	4	31	32
1	1167.590	-3.6	0	1	1	2
2	1167.093	-3.0	0	1	6	7
1	1163.998	0.2	2	3	17	18
1	1162.862	-2.4	0	1	1	0
1	1158.937	2.8	1	2	4	5
1	1158.613	-0.5	2	3	13	14
2	1154.740	0.5	2	3	16	17
1	1154.722	-2.4	0	1	6	5
1	1151.380	1.1	0	1	8	7
1	1150.669	-2.4	3	4	17	18
2	1146.887	0.4	0	1	6	5
1	1146.691	0.0	3	4	14	15
1	1146.263	-2.9	0	1	11	10
1	1143.239	3.1	1	2	5	4
1	1142.796	1.8	0	1	13	12
2	1140.240	-0.5	0	1	10	9
1	1139.941	-1.1	1	2	7	6
1	1138.684	0.5	4	5	18	19
2	1138.548	-0.1	0	1	11	10
1	1138.368	-1.0	3	4	8	9
1	1138.275	-1.1	1	2	8	7
1	1135.705	3.7	0	1	17	16
2	1135.126	-0.2	0	1	13	12
1	1134.904	-2.3	1	2	10	9
1	1134.782	0.8	4	5	15	16
1	1132.083	2.4	0	1	19	18
2	1131.657	1.5	0	1	15	14
1	1131.616	0.7	5	6	23	24
1	1131.486	-0.3	1	2	12	11
1	1130.760	2.0	4	5	12	13
2	1130.666	0.9	1	2	8	7
1	1130.253	1.2	0	1	20	19
2	1128.138	2.0	0	1	17	16
1	1128.017	0.8	1	2	14	13
1	1128.011	1.8	4	5	10	11
1	1127.954	0.2	5	6	20	21
2	1123.970	-1.7	1	2	12	11
1	1123.787	0.3	4	5	7	8
1	1123.561	-2.4	2	3	9	8
1	1120.264	-1.0	5	6	14	15
1	1120.194	-0.7	2	3	11	10
1	1117.593	-1.7	5	6	12	13
1	1117.307	-1.5	1	2	20	19
1	1103.378	-0.6	0	1	34	33

TABLE II. Fitted molecular constants and uncertainties (2σ).

$B_e =$	0.797 940(3) cm <sup>-1</sup>						
$\omega_e =$	1177.7196(8) cm <sup>-1</sup>						
$a_1 =$	-3.0005(2)						
$a_2 =$	5.7000(16)						
$a_3 =$	-8.400(28)						
$a_4 =$	9.47(34)						
$a_5 =$	-7.75(106)						
$a_6 =$	11.72(700)						
Correlation matrix							
$B_e$	$\omega_e$	$a_1$	$a_2$	$a_3$	$a_4$	$a_5$	$a_6$
1.000							
-0.061	1.000						
-0.072	-0.857	1.000					
0.107	0.768	-0.987	1.000				
-0.123	0.872	-0.880	0.845	1.000			
0.082	-0.833	0.908	-0.893	-0.991	1.000		
-0.055	0.742	-0.913	0.929	0.920	-0.956	1.000	
-0.081	0.722	-0.674	0.634	0.879	-0.856	0.678	1.000
Standard deviation of the fit: 0.0021 cm <sup>-1</sup>							

This reduces the number of adjustable parameters for a direct fit of the data to the potential function from eight to three. The residual STD of this fit was 0.07 cm<sup>-1</sup>. The dissociation energy obtained is  $D = 52\,828(50)$  cm<sup>-1</sup> with  $a = -2.870(5)$  (Fig. 3). The uncertainty quoted is only that due to the experimental error and does not include systematic deviations due to the choice of potential, which may be sizable. The Morse potential yields a fairly good fit for only three adjustable parameters, but is clearly unable to reproduce the experimental data within measurement uncertainty, as it does not allow for higher order anharmonicities ( $Y_{n0}, n > 3$ ). The dissociation energy is that to the lowest channel, neglecting the monopole-induced dipole potential for C<sup>+</sup> and Cl at large distances.

The relative intensities of several lines have been measured to allow an estimate of the rotational and vibrational excitation of CCl<sup>+</sup> in the He discharge. The rotational temperature is found to be 540 K ± 30%. The effective vibrational temperature averages at 2000 K but seems to increase with vibrational quantum number, indicating a nonequilibrium vibrational distribution. The effective translational energy of the ions, including the velocity component imparted

TABLE III. Calculated Dunham coefficients for C<sup>35</sup>Cl<sup>+</sup>. Uncertainties are 2σ, all frequencies are in cm<sup>-1</sup>.

$Y_{10}$	1177.716 5(8)
$Y_{20}$	-6.647 5(3)
$Y_{30}$	0.010 08(8)
$Y_{40}$	-9.6(6) 10 <sup>-5</sup>
$Y_{01}$	0.797 940(3)
$Y_{11}$	-0.006 489 3(8)
$Y_{21}$	6.9(4) × 10 <sup>-6</sup>
$Y_{31}$	-1.5(4) × 10 <sup>-7</sup>
$Y_{02}$	-1.465 178(2) × 10 <sup>-6</sup>
$Y_{12}$	-6.238(7) × 10 <sup>-10</sup>
$Y_{22}$	-4.1(7) × 10 <sup>-11</sup>
$Y_{03}$	-1.4(6) × 10 <sup>-15</sup>
$Y_{13}$	6.023(9) × 10 <sup>-13</sup>

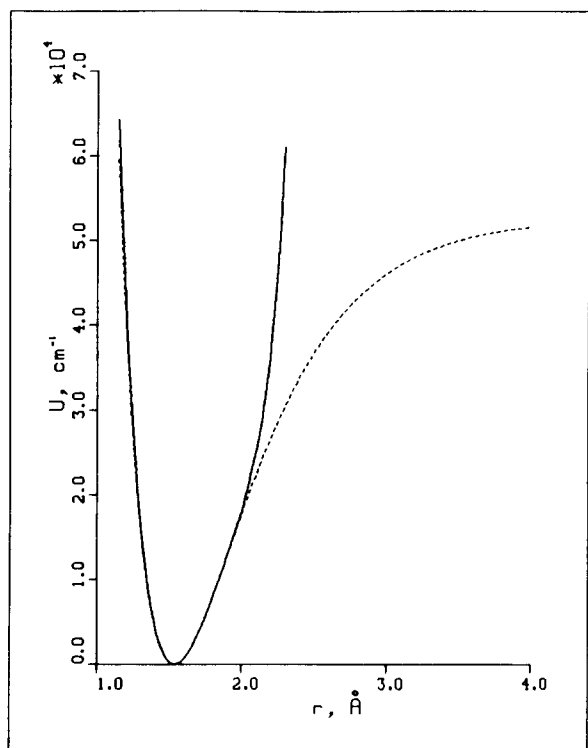


FIG. 3. Potential functions for  $\text{CCl}^+$ ; the solid line represents the power series expansion, the broken line the Morse potential.

by the discharge electric field, was estimated from the linewidth. For a He buffer at 300 K, the Langevin rate constant of  $5.3 \times 10^{-10}$  resulted in a pressure broadening contribution of  $0.0016 \text{ cm}^{-1}$  and an ion translational energy of  $1000 \pm 300 \text{ K}$ . Unlike the case of neutrals, the translational degree of freedom of ions does not serve as a sink for the rotational degree of freedom because it directly receives energy from the discharge electric field. The above estimates were made by assuming that the vibrational dipole moment operator is well represented by the harmonic approximation. In view of the strong repulsive potential, resonant pumping seems unlikely as an explanation of the high excitation. The effect could be due to a combination of nascent excitation upon formation of the small fragments from relatively large

parent species, and slow vibrational deexcitation in the noble gas discharge. This is supported by the apparently nonthermal vibrational population distribution.

Table IV gives a comparison of the  $\text{CCl}^+$  molecular constants with those of the neutral  $\text{CCl}$ , showing the trends expected from molecular orbital theory upon ionization of a  $\pi^*$  electron. Peterson and Woods have recently performed *ab initio* calculations on  $\text{CCl}^+$ <sup>18</sup> using the MP4SDQ method to calculate the potential function, and fitting the results to a sixth order power series expansion similar to the one used in the present study to obtain spectroscopic constants. Their results, which are in excellent agreement with the experimental data, are also summarized in Table IV.

The precise structure determined here should prove useful for the astrophysical detection of  $\text{CCl}^+$ . As Blake, Anicich, and Huntress<sup>20</sup> have shown,  $\text{CCl}^+$  has vanishingly small rate coefficients for reactions with  $\text{H}_2$ ,  $\text{N}_2$ ,  $\text{O}_2$ ,  $\text{CO}$ ,  $\text{CO}_2$ ,  $\text{H}_2\text{O}$ , and  $\text{CH}_4$ , reacting rapidly only with  $\text{O}$ ,  $\text{NH}_3$ , and  $\text{H}_2\text{CO}$ . The dominant loss mechanisms in dense interstellar clouds are therefore likely to be the reaction with atomic oxygen and recombination with electrons.  $\text{CCl}^+$  is formed primarily by the reaction of  $\text{C}^+$  with  $\text{HCl}$ , which has recently been detected in the Orion molecular cloud.<sup>21</sup> Chemical modeling of the chlorine chemistry of dense molecular clouds suggests that detectable amounts of  $\text{CCl}^+$  may exist in such regions if, as has been hypothesized, the gas phase atomic oxygen content is low. The calculated fractional abundances for  $\text{CCl}^+$  in oxygen rich and oxygen poor regions are  $3 \times 10^{-13}$  and  $1.5 \times 10^{-11}$ , respectively. Thus, searches for  $\text{CCl}^+$  will provide information not only about the detailed nature of chlorine chemistry in the interstellar medium, but should also produce valuable insights into the overall chemical balance of dense molecular clouds. For example, the detected  $\text{HCl}$  abundance in OMC-1 is roughly a factor of 2 below that expected from early models of interstellar chlorine chemistry. The detection of  $\text{CCl}^+$  would therefore help determine whether gas phase reaction mechanisms are responsible for the reduced  $\text{HCl}$  abundance or whether grain mantle depletion mechanisms are also important. With a calculated dipole moment of  $0.12 \text{ D}^{18}$  and the fractional abundances noted above,  $\text{CCl}^+$  might be detect-

TABLE IV. Comparison of molecular constants for the  $^{35}\text{Cl}$  substituted species. Uncertainties (where available) are  $2\sigma$ , frequencies in  $\text{cm}^{-1}$ .

Constant	Present study $\text{CCl}^+$	Ref. 18 $\text{CCl}^+$	Ref. 11 <sup>a</sup> $\text{CCl}^+$	Ref. 12 <sup>a</sup> $\text{CCl}^+$	Ref. 19 $\text{CCl}$
$B_e$	0.797 940(3)	0.794	0.6807 <sup>b</sup>	0.8487(8)	0.697 23(8)
$\alpha_e$	0.006 4893(8)	0.00641	...	0.003	0.006 80(2)
$D_e \times 10^{-6}$	1.465 178(2)	1.44	1.15 <sup>b</sup>	2.3	1.48 <sup>c</sup>
$\omega_e$	1177.7196(8)	1178.3	...	1170 <sup>c</sup>	876.746(8)
$\omega_e x_e$	6.6475(3)	6.14	...	5 <sup>c</sup>	5.330(4)
$r_e$	1.537 754(3) <sup>d</sup>	1.541	1.633	1.486	1.6451(1)

<sup>a</sup>No distinction between isotopes.

<sup>b</sup>Values for  $v = 0$ .

<sup>c</sup> $D$  value without further specification.

<sup>d</sup>Bond distances in Å; conversion factor is  $I(\text{Å}^2 \text{amu}) = 16.857 6306/B(\text{cm}^{-1})$  with  $\mu(35) = 8.934 138 34$  and  $\mu(37) = 9.059 177 83 \text{ amu}$ .

<sup>e</sup>Reference 10 quoted in Ref. 12.

able with current millimeter-wave instruments in oxygen deficient clouds, but not in clouds rich with O. The constants of this work predict the  $J = 0 \rightarrow 1$  transitions to lie at 47.649(4) GHz for  $\text{C}^{35}\text{Cl}^+$  and at 46.933(4) GHz for  $\text{C}^{37}\text{Cl}^+$ , well removed from any atmospheric absorption features. This represents the average over the nuclear quadrupole structure of chlorine, which could not be resolved in the present study [Ref. 18 gives a theoretical value of  $eQ_q(\text{Cl}) = -19.8$  MHz].

*Note added in proof:* P. Botschwina at the University of Kaiserslautern has used our potential function to calculate the dipole moment of  $\text{CCl}^+$  at the CEPA-1 level (82 contracted GTO's) to be 0.11 D with the negative center on the carbon, in good agreement with Ref. 18. The "reversed" dipole found in CO apparently also occurs in charged halocarbon analogs. The transition dipole moment is calculated to be  $-0.26$  D, making  $\text{CCl}^+$  a strong absorber.

#### ACKNOWLEDGMENTS

This work was supported by a grant from IBM Corporation, the National Science Foundation Presidential Young Investigator Program (Grant No. CHE-8351885) and the NSF Structure and Thermodynamics Program (Grant No. CHE-8402861). The authors would also like to thank Edward Yang, for assistance with data collection. MG would like to thank the University of California for a fellowship and GAB would like to thank the Miller Research foundation for support. Finally, we are indebted to Professor K. N. Rao for

making  $\text{NH}_3$  calibration spectra available to us before publication, and to Anthony Young and H. S. Johnston for providing one of the diodes used in this study.

- <sup>1</sup>J. W. Cobourn and H. F. Winters, *J. Vac. Sci. Technol.* **16**, 391 (1979).
- <sup>2</sup>D. C. Hovde, E. Schaefer, S. E. Strahan, C. A. Ferrari, D. Ray, K. G. Lubic, and R. J. Saykally, *Mol. Phys.* **52**, 245 (1984).
- <sup>3</sup>D. Ray, K. Lubic, and R. J. Saykally, *Mol. Phys.* **46**, 217 (1982).
- <sup>4</sup>K. G. Lubic, D. Ray, L. Veseth, and R. J. Saykally (in preparation).
- <sup>5</sup>E. Schaefer and R. J. Saykally, *J. Chem. Phys.* **81**, 4189 (1984).
- <sup>6</sup>M. Gruebele, M. Polak, and R. J. Saykally, *Chem. Phys. Lett.* **125**, 165 (1986).
- <sup>7</sup>K. Kawaguchi and E. Hirota, *J. Chem. Phys.* **83**, 1437 (1985).
- <sup>8</sup>K. Kawaguchi and E. Hirota, *J. Chem. Phys.* **84**, 2953 (1986).
- <sup>9</sup>R. F. Barrow, G. Drummond, and S. Walker, *Proc. Phys. Soc. London Sect. A* **67**, 186 (1954).
- <sup>10</sup>Yu. Ya. Kuzyakov and V. M. Tatevsky, *Nauchn. Dokl. Vys. Sck. Khim. Khim. Tekhnol.* **2**, 237 (1959).
- <sup>11</sup>R. D. Verma, *J. Mol. Spectrosc.* **7**, 145 (1961).
- <sup>12</sup>H. Bredohl, I. Dubois, and F. Melen, *J. Mol. Spectrosc.* **98**, 495 (1983).
- <sup>13</sup>G. Guelachvili, *Can. J. Phys.* **60**, 1334 (1982).
- <sup>14</sup>K. N. Rao (private communication).
- <sup>15</sup>C. S. Gudemann and R. J. Saykally, *Annu. Rev. Phys. Chem.* **35**, 387 (1984).
- <sup>16</sup>J. L. Dunham, *Phys. Rev.* **41**, 721 (1932).
- <sup>17</sup>G. M. Plummer, T. Anderson, E. Herbst, and F. C. deLucia, *J. Chem. Phys.* **84**, 2427 (1986).
- <sup>18</sup>K. Peterson and R. C. Woods (to be published).
- <sup>19</sup>C. Yamada, K. Nagai, and E. Hirota, *J. Mol. Spectrosc.* **85**, 416 (1981).
- <sup>20</sup>G. A. Blake, V. G. Anicich, and W. T. Huntress, *Astrophys. J.* **300**, 415 (1986).
- <sup>21</sup>G. A. Blake, J. Keene, and T. G. Phillips, *Astrophys. J.* **295**, 501 (1985).